HIGH-RESOLUTION OBSERVATIONS OF CO TOWARD MASSIVE YOUNG STELLAR OBJECTS: INVESTIGATIONS OF PROTOPLANTETARY CARBON AND OXYGEN IN THE GALAXY. Rachel L. Smith[1,2], Geoffrey A. Blake[3], A. C. Adwin Boogert[4], Klaus M. Pontoppidan[5], Alexandra C. Lockwood[6], [1]North Carolina Museum of Natural Sciences (rachel.smith@naturalsciences.org), [2]Appalachian State University, Department of Physics and Astronomy, [3]California Institute of Technology, Division of Geological and Planetary Sciences,[4]SOFIA/USRA, NASA Ames, [6]King Abdullah University of Science and Technology.

Introduction: High-resolution near-infrared observations of carbon monoxide (CO) gas in absorption have been shown to enable precise comparisons between carbon and oxygen isotopic reservoirs toward low-mass (solar-type) young stellar objets (YSOs) within $\sim$ 1 kiloparsec (kpc) of the Sun [1-3]. Results with such observations have revealed signatures of CO self shielding – supportive evidence for this process on disk surfaces [2,3,4] – and significant heterogeneity in [^{12}CO]/[^{13}CO], with possible interplay between CO ice and gas reservoirs as a cause [3,5,6]. Precise ratios of [^{12}C^{18}O]/[^{12}C^{17}O] have also been used to argue for supernova enrichment in the early solar system [7], and comparison between low-mass binary systems and embedded protostars suggest carbon isotopic homogeneity within a few hundred AU [8].

Here we present results from our ongoing observational survey of CO isotopologues toward massive YSOs along a galactic gradient. Unlike their low-mass counterparts, massive YSOs are observational tracers of regions with high-UV fluxes, span a larger observational range in Galactocentric radius ($R_{\rm GC}$), and enable robust comparisons to other carbon reservoirs along the same lines of sight. These targets thereby provide robust observational comparisons with solar-type YSOs, helping to shed light on key chemical reservoirs involved protoplanetary and prebiotic evolutionary pathways.

Observations and Methods: We have thus far observed 14 massive YSO targets with Keck-NIRSPEC (R$\sim 25,000$). Targets span in $R_{\rm GC}$ from 4.5 to 9.7 kpc and range in luminosity from $\sim 1{\times}10^3$ to $\sim 4.7{\times}10^5$ $L_{\rm Sun}$. Fundamental ($v = 1{-}0$) and first overtone ($v = 2 - 0$) rovibrational spectra were reduced using our customized IDL pipeline (example, Figure 1). Equivalent widths (W_ν) for each isotopologue line were computed using polynomial + Gaussian fits (sample fits, Figure 1). For ^{12}C^{18}O and ^{12}C^{17}O lines, column densities (N_J) were calculated directly using the optically thin relation, $W_\nu = (\pi e^2/m_e c^2) f_J N_J$ [9], with f_J representing the absorption oscillator strength for the $J^{\rm th}$ transition. A curve of growth (example, Figure 2, top) relating W_ν to N_J, was used in conjunction with a rotational analysis (example, Figure 2, bottom) to find the best-fit Doppler broadening parameter (b) for each YSO; this b was then used to derive N_J values for the ^{12}CO and ^{13}CO lines. Total column densities for each isotopologue were then found using the best-fit b and the derived rotational temperatures.

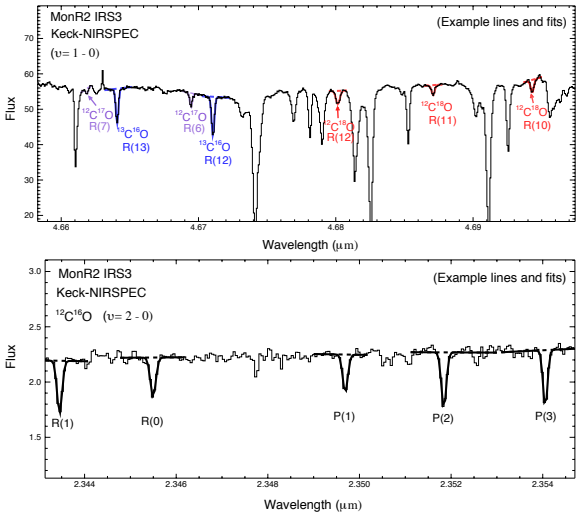

Figure 1: Portions of CO fundamental rovibrational spectra for massive YSO, MonR2 IRS3. Representative absorption lines are marked. Colored model fits are shown overlaid on the spectral lines. (Top): Fundamental band ($v = 1 - 0$) band. (Bottom): First overtone ($v = 2 - 0$) band; several optically thin ^{12}CO lines are marked.

Results and discussion: Derived ratios of [^{12}CO]/[^{13}CO] for the four fully analyzed massive YSOs thus far – AFGL 2136 [10], MonR2 IRS3, NGC 7538 IRS9, and W3 IRS5; $R_{\rm GC}$ from 6.1 to 9.7 kpc – are shown in Figure 3, which plots ^{12}C/^{13}C against $R_{\rm GC}$. For the massive YSOs, we find that the [^{12}CO]/[^{13}CO] derived from the cold gas (T $\sim$5 to 60 K) consistently follows the predicted Galactic trend for [^{12}C/^{13}C], unlike the significant dispersion previously found in the low-mass sources at $\sim$ 8 kpc [3,8]. Further, the cold-gas [^{12}CO]/[^{13}CO] are consistently lower than the solid-phase [^{12}CO$_2$]/[^{13}CO$_2$] [11] for the same lines of sight, which suggests that CO$_2$ may not originate directly from CO reservoirs as previously assumed [12]. For massive YSOs with two-temperature distributions, warm-gas [^{12}CO]/[^{13}CO] ratios are consistently higher than those from the cold gas, a trend we also see in the low-mass targets, suggesting that there may be similar temperature-dependent CO fractionation pathways for both high- and low-mass YSOs. Our [^{12}CO]/[^{13}CO] ratio for W3 IRS5 (103 ± 4) is significantly higher than that derived from radio observations of ^{12}C^{18}O

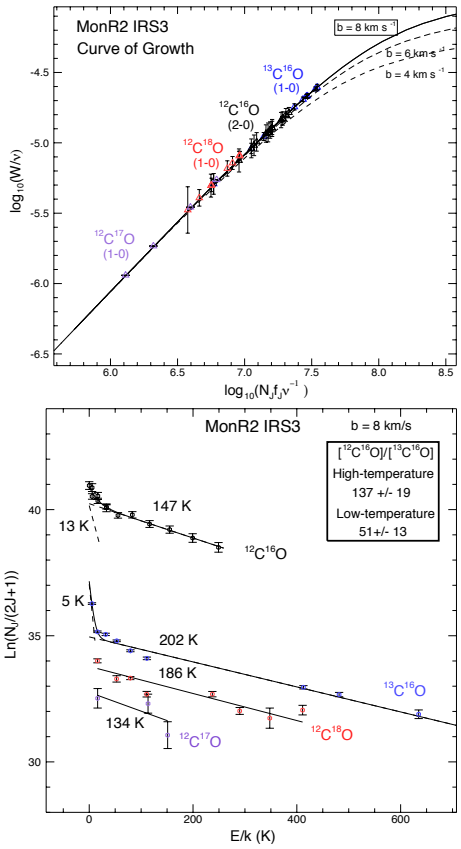

Figure 2: Analysis for massive YSO MonR2 IRS3. (Top): Curve of growth showing the best-fit b value (8 km/s), as well as other nearby values for comparison. (Bottom): Rotational analysis for MonR2 IRS3. Error bars are 1σ, E_J is the energy of the J^{th} rotational state, k is the Boltzmann constant.

and the doubly-substituted $^{13}C^{18}O$ (66 ± 4) [13]. This discrepancy could be due to a higher photodissociation rate for $^{12}C^{18}O$ [14]. We find a mass-independent trend in oxygen isotopes for W3 IRS5 (Figure 4), suggesting that CO self-shielding could affect the evolution of oxygen isotopes in protoplanetary disks surrounding both massive and solar-type YSOs.

Conclusions: Our high-resolution observations of CO toward massive YSOs across the Galaxy thus far show ratios $[^{12}CO]/[^{13}CO]$ with significantly less dispersion off the predicted Galactic trend than low-mass YSOs. We find signatures of CO self-shielding in both high- and low-mass YSOs, and similar trends between beteween CO ice and gas reservoirs. Together, our results suggest that massive YSOs may follow dissimilar pathways in certain phases of evolution in protoplanetary carbon and oxygen as compared to solar-type systems. Further, our observational suggestion that CO_2 may not originate from CO should be considered in evaluating carbon-based pathways for protoplanetary and prebiotic compounds.

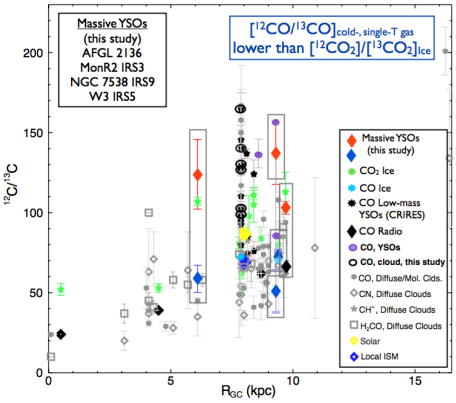

Figure 3: Ratios of $^{12}C/^{13}C$ vs. R_{GC} (kpc) for our massive YSOs in this study (boxed, R_{GC}~6 to 10 kpc), data from the literature [15-19], and CO_{Gas} from the high-resolution CRIRES survey at $\sim$ 8 kpc [2,3,8]. Massive YSO warm- and cold-gas values are shown as red and blue diamonds, respectively. CO_2 ice values are green stars [9]. Local ISM ($\sim$ 68) and solar system ($\sim$ 87) values are also at $\sim$ 8 kpc.

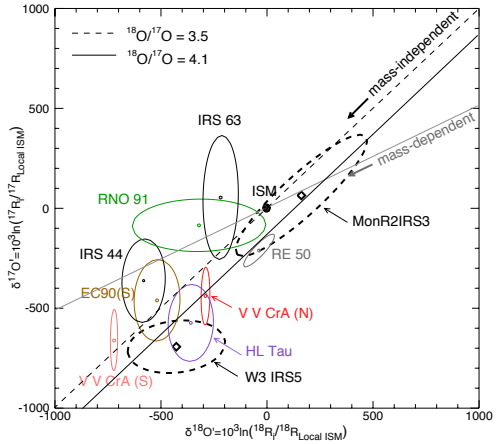

Figure 4: Three-isotope oxygen plot showing low- and high-mass YSOs compared to the ISM. Mass-independent trends are seen in the low-mass YSOs VV CrA(N) and HL Tau [3], and the massive YSO W3 IRS5. Error ellipses are $1-\sigma$.

References: [1]Brittain S.D. et al. (2005) *ApJ 626*, 283-291.[2]Smith R.L. et al. (2009) *ApJ 701*, 163-175.[3]Smith R.L. et al. *ApJ 813*, 120-135.[4]Lyons J.R. and Young E.D. (2005) *Nature 435, 7040*, 317- 320.[5]Pontoppidan K.M. (2006) *A&A 453*, L47.[6]Young E.D. and Schauble E.A. *42nd LPI, 1608*, 1323.[7]Young E.D. et al. (2011) *ApJ, 729*, 43.[8]Smith R.L. et al. (2013) *44th LPI, 1719*, 2698.[9]Spitzer L. J. (1978) Physical Processes in the Interstellar Medium.[10]Smith R.L. et al. *78th Metsoc, 1856*, 5385.[11]Boogert A.C.A. et al. (2000) *A&A 353*, 349-362.[12]van Dishoeck E.F. et al. (1996) *A&A 315*, L349-352.[13]Langer W.D. and Penzias A. A. (1990) *ApJ 357*, 477-492.[14] van Dishoeck E. F. and Black J. H. (1988) *ApJ 334* 771-802.[15]Milam S.N. et al. (2005) *ApJ 634*, 1126-1132.[16]Scott P.C. et al. (2006) *A&A. 456*, 675-688.[17] Goto M. et al. (2003) *ApJ 598*, 1038-1047.[18]Federman S.R. et al. (2003) *ApJ 591*, 989-999.[19]Lambert D.L. et al. (1994) *ApJ 420*, 756-771.